III International Conference on Particle-based Methods – Fundamentals and Applications
PARTICLES 2013
M. Bischoff, E. Oñate, D.R.J. Owen, E. Ramm & P. Wriggers (Eds)

A MODIFIED FINITE PARTICLE METHOD: MULTI-DIMENSIONAL STATICS AND DYNAMICS

DOMENICO ASPRONE[1], FERDINANDO AURICCHIO[2,3], ANDREA MONTANINO[2,3] AND ALESSANDRO REALI[2,3]

[1] Dipartimento di Ingegneria Strutturale (DIST)
Università degli Studi di Napoli, via Claudio 21, 80125 Napoli (Italy)

[2] Dipartimento di Ingegneria Civile ed Architettura (DICAr)
Università degli Studi di Pavia, via Ferrata 3, 27100 Pavia (Italy)

[3] Centro di Simulazione Numerica Avanzata (CeSNA)
Istituto Universitario di Studi Superiori, piazza della Vittoria 15, 27100 Pavia (Italy)

Key words: Particle methods, collocation methods, projection methods, elasto-dynamics

Abstract. We present the so-called Modified Finite Particle Method (MFPM), that is a recent methodology of approximation of differential operators, based on the projection of the Taylor series of a function $u(x)$ on a set of projection functions.

In particular, we discuss the generalization of MFPM formulation to the multi-dimensional case, extending the methodological procedure adopted for the one-dimensional case. Moreover, we address the extension to dynamics and solve problems with an explicit time integration scheme. Finally, we apply the MFPM to an elasto-statics (a perforated plate under tension) and two elasto-dynamics (a two-dimensional bar under a quasi-impulsive load and a quarter of an annulus under a sinusoidal body load) benchmarks. When an analytical solution is available we calculate the corresponding convergence orders of the error, always obtaining the expected second-order accuracy

1 INTRODUCTION

In recent years, meshless numerical methods have become increasingly important due to their characteristic of being totally free of grids or meshes. This is particularly useful when dealing with the numerical simulation of problems implying large deformations or high velocity impacts, where classical element-based methods (e.g., the Finite Element Method) suffer from pathologies like excessive element distortion, spurious numerical errors, and mesh sensitivity. On the contrary, meshless methods overcome these difficulties since the nodes are not "rigidly" connected between themselves. As a consequence, the approximation is carried out taking into account the current distribution of the particles.

Among meshless methods, we focus in particular on Particle Methods. The first proposed particle method has been the Smoothed Particle Hydrodynamics (SPH), introduced by Lucy [1] and Gingold and Monaghan [2], for the study of astrophysical problems. In this method the whole domain Ω is discretized in a finite number of particles, each one characterized by a given mass, velocity, and energy. Therefore the state of a continuum is represented by the properties of the particles, and as a consequence SPH is particularly suitable for the description of the behaviour of fluids and ideal gases. The starting point, in 1D, is the identity

$$f(x_i) = \int_\Omega f(x)\delta(x - x_i)\, dx \tag{1}$$

where $\delta(x - x_i)$ is the Dirac Delta function. The first approximation consists of replacing the Dirac Delta function with a bell-shaped smooth function $W(x-x_i, h)$, called *smoothing function* or *kernel function*:

$$f(x_i) \simeq \int_\Omega f(x)W(x - x_i, h)\, dx \tag{2}$$

then the derivatives are computed according to

$$f^{(n)}(x_i) \simeq (-1)^n \int_\Omega f(x)W^{(n)}(x - x_i)\, dx \tag{3}$$

Equation (2) is referred as the *kernel evaluation* of $f(x)$. The amount h is the *smoothing length*, that is the distance where the smoothing function is significantly different from zero. In order to numerically evaluate the integrals of Equations (2) and (3), the whole domain is divided into a number of subdomains, each associated to a particle x_j; then the integrals are replaced by summations over j.

In proximity of the boundary, Equations (2) and (3) are inaccurate because the smoothing function is not completely developed: as a consequence, many other method have been developed to overcome this deficiency.

One of the first has been introduced by Liu et al. [3], that introduced a polynomial corrective function in order to restore the effectiveness of Equation (2) also at the boundary, but leaving unsolved the inaccuracy of Equation (3). Chen et al. [4], in the Corrective Smoothed Particle Method (CSPM) achieve accurate formulas for the kernel evaluation by manipulating Taylor series expansion up to the zero-th order, then the following approximations are carried out by considering the following terms of the Taylor series, and using the previous approximations. In the Modified Smoothed Particle Hydrodynamics (MSPH) [5], the unknown function and its derivatives are evaluated at the same time. This procedure prevents the method from error propagation, but increases the computational cost, since at each particle a system of equations has to be solved.

In Asprone et al. [6] a Modified Finite Particle Method (MFPM) has been developed starting from the MSPH [5]. The kernel evaluation of the unknown function is not computed, since it is assumed that the value of the function is not a real unknown of the problem. Moreover a 1D elasto-statics test is solved using this method as well as others taken from the literature (the original SPH formulation [1], the RKPM [3], the CSPM [4]) and the results are compared. In Asprone et al. [7] MFPM is extended to a 2D scalar problem, while in Asprone et al. [8] the solution of some 2D elasto-statics and elasto-plastics problems are presented.

In this work we recall the 1D formulation of MFPM. We introduce the extension of the MFPM to the multi-dimensional case, and give an analytical expression of the discrete form of the differential operators, then we recall the equations of structural elasto-dynamics and show their discrete form by MFPM, then we show the treatment of the boundary conditions for explicit time integration. We apply the method to some elasto-statics and elasto-dynamics tests. Finally we draw some conclusions and illustrate the further developments of the method.

2 MODIFIED FINITE PARTICLE METHOD: MULTI-DIMENSIONAL FORMULATION

In the following we show the extension of the Modified Finite Particle Method to the three-dimensional case, recalling the same steps of the 1D procedure presented in Asprone et al. [6].

We consider the Taylor series expansion of an unknown function $u(\boldsymbol{x})$ up to the second order and multiply it by 9 *projection functions* $W_i^k = W^k(\boldsymbol{x} - \boldsymbol{x}_i)$, $k = 1, ..., 9$; then, integrating over the domain, we obtain a set of equations of the type

$$
\begin{aligned}
& D_x u(\boldsymbol{x}_i) \int_\Omega (x - x_i) W_i^k \, dV + D_y u(\boldsymbol{x}_i) \int_\Omega (y - y_i) W_i^k \, dV + D_z u(\boldsymbol{x}_i) \int_\Omega (z - z_i) W_i^k \, dV + \\
& \frac{1}{2} D_{xx}^2 u(\boldsymbol{x}_i) \int_\Omega (x - x_i)^2 W_i^k \, dV + \frac{1}{2} D_{yy}^2 u(\boldsymbol{x}_i) \int_\Omega (y - y_i)^2 W_i^k \, dV + \\
& \frac{1}{2} D_{zz}^2 u(\boldsymbol{x}_i) \int_\Omega (z - z_i)^2 W_i^k \, dV + D_{xy}^2 u(\boldsymbol{x}_i) \int_\Omega (x - x_i)(y - y_i) W_i^k \, dV + \\
& D_{yz}^2 u(\boldsymbol{x}_i) \int_\Omega (y - y_i)(z - z_i) W_i^k \, dV + D_{xz}^2 u(\boldsymbol{x}_i) \int_\Omega (x - x_i)(z - z_i) W_i^k \, dV = \\
& \int_\Omega (u(\boldsymbol{x}) - u(\boldsymbol{x}_i)) W_i^k \, dV
\end{aligned}
\tag{4}
$$

that can be rewritten in matrix form as:

$$\boldsymbol{A}_i \begin{pmatrix} D_x u(\boldsymbol{x}_i) \\ D_y u(\boldsymbol{x}_i) \\ D_z u(\boldsymbol{x}_i) \\ D^2_{xx} u(\boldsymbol{x}_i) \\ D^2_{yy} u(\boldsymbol{x}_i) \\ D^2_{zz} u(\boldsymbol{x}_i) \\ D^2_{xy} u(\boldsymbol{x}_i) \\ D^2_{yz} u(\boldsymbol{x}_i) \\ D^2_{xz} u(\boldsymbol{x}_i) \end{pmatrix} = \begin{pmatrix} \int_\Omega \left(u(\boldsymbol{x}) - u(\boldsymbol{x}_i)\right) W_i^1 \, dV \\ \int_\Omega \left(u(\boldsymbol{x}) - u(\boldsymbol{x}_i)\right) W_i^2 \, dV \\ \int_\Omega \left(u(\boldsymbol{x}) - u(\boldsymbol{x}_i)\right) W_i^3 \, dV \\ \int_\Omega \left(u(\boldsymbol{x}) - u(\boldsymbol{x}_i)\right) W_i^4 \, dV \\ \int_\Omega \left(u(\boldsymbol{x}) - u(\boldsymbol{x}_i)\right) W_i^5 \, dV \\ \int_\Omega \left(u(\boldsymbol{x}) - u(\boldsymbol{x}_i)\right) W_i^6 \, dV \\ \int_\Omega \left(u(\boldsymbol{x}) - u(\boldsymbol{x}_i)\right) W_i^7 \, dV \\ \int_\Omega \left(u(\boldsymbol{x}) - u(\boldsymbol{x}_i)\right) W_i^8 \, dV \\ \int_\Omega \left(u(\boldsymbol{x}) - u(\boldsymbol{x}_i)\right) W_i^9 \, dV \end{pmatrix} \tag{5}$$

The choice of the *projection functions* is performed with the only requirement that, at each particle, the matrix $\boldsymbol{A}_i$ is non singular. In our tests we choose

$$\begin{cases} W_i^1 = x - x_i \\ W_i^2 = y - y_i \\ W_i^3 = z - z_i \end{cases} \qquad \begin{cases} W_i^4 = (x - x_i)^2 \\ W_i^5 = (y - y_i)^2 \\ W_i^6 = (z - z_i)^2 \end{cases} \qquad \begin{cases} W_i^7 = (x - x_i)(y - y_i) \\ W_i^8 = (y - y_i)(z - z_i) \\ W_i^9 = (x - x_i)(z - z_i) \end{cases}$$

The domain is divided into finite subdomains ΔV_j, one for each particle $\boldsymbol{x}_j$, according to the Voronoi tessellation procedure; for each particle an influence region Ω_i is also defined, depending, in SPH-based methods, on the *smoothing length*. In MFPM we do not define a fixed value of the smoothing length, but we prefer to set the number of particles to be considered for the approximation of derivatives. For all the particles such that $x_j \notin \Omega_i$ we pose that $W_i^k(\boldsymbol{x} = \boldsymbol{x}_j) = 0$ for all $k = 1, ..., 9$. Then, the integrals are approximated with summations, and the approximation schemes for the first and second spatial derivatives at each particle x_i are obtained by inverting (5).

Therefore, we are able to write the analytical approximation schemes of the spatial derivatives. In particular, the approximation schemes of the first derivatives are:

$$\begin{cases} D_{x,ij} = \displaystyle\sum_{k=1}^{9} E^i_{1k} \left[W^k_{ij} \Delta V_j - \delta_{ij} \sum_h W^k_{ih} \Delta V_h \right] \\ D_{y,ij} = \displaystyle\sum_{k=1}^{9} E^i_{2k} \left[W^k_{ij} \Delta V_j - \delta_{ij} \sum_h W^k_{ih} \Delta V_h \right] \\ D_{z,ij} = \displaystyle\sum_{k=1}^{9} E^i_{3k} \left[W^k_{ij} \Delta V_j - \delta_{ij} \sum_h W^k_{ih} \Delta V_h \right] \end{cases} \tag{6}$$

and the schemes for the second derivatives are:

$$\begin{cases} D^2_{xx,ij} = \sum_{k=1}^{9} E^i_{4k} \left[W^k_{ij} \Delta V_j - \delta_{ij} \sum_h W^k_{ih} \Delta V_h \right] \\ D^2_{yy,ij} = \sum_{k=1}^{9} E^i_{5k} \left[W^k_{ij} \Delta V_j - \delta_{ij} \sum_h W^k_{ih} \Delta V_h \right] \\ D^2_{zz,ij} = \sum_{k=1}^{9} E^i_{6k} \left[W^k_{ij} \Delta V_j - \delta_{ij} \sum_h W^k_{ih} \Delta V_h \right] \\ D^2_{xy,ij} = \sum_{k=1}^{9} E^i_{7k} \left[W^k_{ij} \Delta V_j - \delta_{ij} \sum_h W^k_{ih} \Delta V_h \right] \\ D^2_{yz,ij} = \sum_{k=1}^{9} E^i_{8k} \left[W^k_{ij} \Delta V_j - \delta_{ij} \sum_h W^k_{ih} \Delta V_h \right] \\ D^2_{xz,ij} = \sum_{k=1}^{9} E^i_{9k} \left[W^k_{ij} \Delta V_j - \delta_{ij} \sum_h W^k_{ih} \Delta V_h \right] \end{cases} \tag{7}$$

where $\boldsymbol{E}^i$ is the inverse of $\boldsymbol{A}_i$

A 2D formulation of the method is simply achieved by considering only the derivatives in the x and y directions, and $k = 1, 2, 4, 5, 7$ from equation (4) to equation (7). The three-dimensional subdomains ΔV_j are replaced by planar subdomains ΔA_j.

3 ELASTICITY

In the following we introduce the linear elasto-dynamics problem in the three-dimensional space and show how it can be approximated with the Modified Finite Particle Method.

We consider an elastic body on a domain Ω, subjected to internal forces $\boldsymbol{b}$, constrained displacements $\bar{\boldsymbol{s}}$ on the Dirichlet boundary Γ_D and the traction $\bar{\boldsymbol{t}}$ on the Neumann boundary Γ_N.

The equations that govern the problem are

$$\begin{cases} \rho \dfrac{\partial^2 \boldsymbol{s}}{\partial t^2} = & \nabla \cdot \boldsymbol{\sigma} + \boldsymbol{b} & \boldsymbol{x} & \in \Omega \\ \boldsymbol{\sigma n} = & \bar{\boldsymbol{t}}(t) & \boldsymbol{x} & \in \Gamma_N \\ \boldsymbol{s} = & \bar{\boldsymbol{s}}(t) & \boldsymbol{x} & \in \Gamma_D \\ \boldsymbol{s}(\boldsymbol{x}, 0) = & \boldsymbol{s}_0(\boldsymbol{x}) & \boldsymbol{x} & \in \Omega \\ \dfrac{\partial \boldsymbol{s}}{\partial t}(\boldsymbol{x}, 0) = & \dot{\boldsymbol{s}}_0(\boldsymbol{x}) & \boldsymbol{x} & \in \Omega \end{cases} \tag{8}$$

where ρ is the mass density of the material, $\boldsymbol{n}$ is the outward normal vector at the boundary, $\boldsymbol{s} = \boldsymbol{s}(\boldsymbol{x}, t)$ is the vectorial displacement field, whose components are $u = u(\boldsymbol{x}, t)$,

$v = v(\boldsymbol{x}, t)$ and $w = w(\boldsymbol{x}, t)$, $\boldsymbol{\sigma} = \mathbb{C}(\nabla \boldsymbol{s})^S$ is the symmetric Cauchy stress tensor, $\mathbb{C}$ is the fourth order linear elastic isotropic tensor, with components

$$\mathbb{C}_{ijkl} = \lambda \delta_{ij} \delta_{kl} + \mu(\delta_{ik}\delta_{jl} + \delta_{il}\delta_{jk}) \tag{9}$$

where λ and μ are the Lamé constants, which can be expressed in terms of the Young modulus E and the Poisson ratio ν.

By making explicit Equation (8) with respect to the components of the displacement u, v and w, we obtain

$$\begin{cases} \rho u,_{tt} = & (\lambda + 2\mu) u,_{xx} + \mu(u,_{yy} + u,_{zz}) + (\lambda + \mu)(v,_{xy} + w,_{xz}) + b_x \\ \rho v,_{tt} = & (\lambda + 2\mu) v,_{yy} + \mu(v,_{xx} + v,_{zz}) + (\lambda + \mu)(u,_{xy} + w,_{yz}) + b_y \\ \rho w,_{tt} = & (\lambda + 2\mu) w,_{zz} + \mu(w,_{xx} + w,_{yy}) + (\lambda + \mu)(u,_{xz} + v,_{yz}) + b_z \end{cases} \tag{10}$$

where the subscripts preceded by a comma stand for the operation of partial derivative. In the spirit of collocation methods, we enforce the discrete form of Equation (10) for internal particles, and the discrete form of the boundary conditions on the boundary particles, according to the approximation schemes (6) and (7). We obtain a linear system in the form

$$\boldsymbol{K}\hat{\boldsymbol{s}} = \boldsymbol{f} \tag{11}$$

where the components of $\boldsymbol{f}$ are $\rho\ddot{\hat{\boldsymbol{s}}} - \boldsymbol{b}$ for the rows associated to internal particles, and $\bar{\boldsymbol{s}}$ or $\bar{\boldsymbol{t}}$ in case of Dirichlet or Neumann boundary particles respectively.

For elasto-statics applications, the form (11) is sufficient to solve the problem: in this case the time derivative is zero, and the system can be inverted; therefore both the internal and external particle values are found at once.

In case of elasto-dynamics, we have to discretize also the time derivative. We choose an explicit second order scheme

$$\ddot{\hat{\boldsymbol{s}}}^n = \frac{\hat{\boldsymbol{s}}^{n+1} - 2\hat{\boldsymbol{s}}^n + \hat{\boldsymbol{s}}^{n-1}}{\Delta t^2} \tag{12}$$

where Δt is the time step. The equations of the system (11), collocated on internal particles, become

$$\sum_j K_{ij} \hat{s}_j^n = \rho \frac{\hat{s}_i^{n+1} - 2\hat{s}_i^n + \hat{s}_i^{n-1}}{\Delta t^2} - b_i^n \tag{13}$$

while the equations collocated on boundary particles, that do not undergo the time derivative, are in the form

$$\sum_j K_{ij} \hat{s}_j^{n+1} = \bar{u}_i^{n+1} \tag{14}$$

Equations (14) cannot be solved by explicit time integration, since the values of $\hat{s}_j^{n+1}$ may depend, in case of Neumann boundary conditions, on the values of the internal particles at the same time step $n+1$. To overcome this difficulty, we perform a static condensation of $\boldsymbol{K}$, and separate the equations collocated on internal particles from the ones collocated on the boundary. Even the degrees of freedom are separated, and so the final form of Equation (11) is

$$\begin{pmatrix} \boldsymbol{K}_{II} & \boldsymbol{K}_{IB} \\ \boldsymbol{K}_{BI} & \boldsymbol{K}_{BB} \end{pmatrix} \begin{pmatrix} \hat{\boldsymbol{s}}_I \\ \hat{\boldsymbol{s}}_B \end{pmatrix} = \begin{pmatrix} \rho\ddot{\hat{\boldsymbol{s}}}_I - \boldsymbol{b}_I \\ \bar{\boldsymbol{u}} \end{pmatrix} \tag{15}$$

where $\bar{\boldsymbol{u}}$ is the vector of the imposed displacements or the imposed stresses at the boundary, and $\boldsymbol{K}_{II}$, $\boldsymbol{K}_{IB}$, $\boldsymbol{K}_{BI}$, $\boldsymbol{K}_{BB}$ are the minors of the matrix $\boldsymbol{K}$ related to the internal and boundary particles.

From the second set of equations of (15) we compute

$$\boldsymbol{u}_B = \boldsymbol{K}_{BB}^{-1}(\bar{\boldsymbol{u}} - \boldsymbol{K}_{BI}\hat{\boldsymbol{s}}_I) \tag{16}$$

then we replace it into the first set of (15), and obtain

$$(\boldsymbol{K}_{II} - \boldsymbol{K}_{IB}\boldsymbol{K}_{BB}^{-1}\boldsymbol{K}_{BI})\hat{\boldsymbol{s}}_I = \rho\ddot{\hat{\boldsymbol{s}}}_I - \boldsymbol{K}_{IB}\boldsymbol{K}_{BB}^{-1}\bar{\boldsymbol{u}} - \boldsymbol{b}_I \tag{17}$$

where the amount $\boldsymbol{K}_{II} - \boldsymbol{K}_{IB}\boldsymbol{K}_{BB}^{-1}\boldsymbol{K}_{BI}$ is the modified stiffness matrix, namely $\tilde{\boldsymbol{K}}$.

Equations (17) form an unconstrained ordinary differential equation system which can be solved with a suitable time integration scheme, even explicit, (e.g. Equation (12)), taking care to respect the eventual limitations of the time step. The unknowns of this system are the values of the unknown functions at the internal particles.

Equation (16) can be used to retrieve the values of the functions at the boundary particles.

4 APPLICATIONS

In the following we apply the mmethod presented in the earlier sections. First we introduce a 2D statics problem, that is, the classical test of an infinitely extended plate with a central hole under a uniform remote stress. Regarding dynamics problems, we show the wave propagation in a two-dimensional bar, and a quarter of annulus under a sinusoidal body load.

4.1 A quarter of perforated plate

The geometry of this problem is depicted in Figure 1. The radius of the internal hole is $a = 0.2$

The equations that govern the problem are the 2D statics version of (10). The boundary conditions are

$$\begin{cases} \boldsymbol{\sigma n} = \boldsymbol{0} & \text{on } \Gamma_1 \text{ and } \Gamma_4 \\ \boldsymbol{\sigma n}\cdot\boldsymbol{t} = 0 \quad \text{and} \quad \boldsymbol{s}\cdot\boldsymbol{n} = 0 & \text{on } \Gamma_2 \text{ and } \Gamma_5 \\ \boldsymbol{\sigma n} = [\sigma_0 \quad 0]^T & \text{on } \Gamma_3 \end{cases} \tag{18}$$

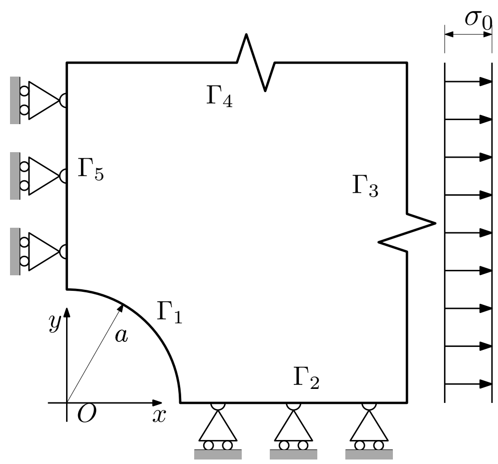

Figure 1: The model of a quarter of square plate with a central hole

where $\boldsymbol{n}$ is the outward normal, $\boldsymbol{t}$ is the unit vector tangent to the boundary, and σ_0 is the remote stress.

We solve the problem considering a reduced domain, on which we impose boundary conditions according to the exact solution, that is, in terms of stresses,

$$\sigma_{xx} = \sigma_0 \left[1 - \frac{a^2}{r^2} \left(\frac{3}{2} \cos 2\theta + \cos 4\theta \right) + \frac{3a^4}{2r^4} \cos 4\theta \right] \tag{19a}$$

$$\tau_{xy} = \sigma_0 \left[-\frac{a^2}{r^2} \left(\frac{1}{2} \sin 2\theta + \sin 4\theta \right) + \frac{3a^4}{2r^4} \sin 4\theta \right] \tag{19b}$$

$$\sigma_{yy} = \sigma_0 \left[-\frac{a^2}{r^2} \left(\frac{1}{2} \cos 2\theta - \cos 4\theta \right) - \frac{3a^4}{2r^4} \cos 4\theta \right] \tag{19c}$$

where (r, θ) are the polar coordinates, θ being measured from the positive x-axis counter-clockwise.

We introduce the Stress Intensity Factor (SIF), that is the ratio between the maximum σ_{xx} and the remote stress σ_0. For the test under consideration, the analytical solution provides $SIF = 3$. We solve the problem with the following values of the data

$$E = 100000\,, \quad \nu = 0.33\,, \quad \sigma_0 = 100 \tag{20}$$

and then we compare the analytical value of the SIF with the numerical results. The distribution of σ_{xx} stress is shown in Figure 2(a). The error is computed as

$$e_r = \frac{|SIF_{an} - SIF_{num}|}{|SIF_{an}|} = \frac{|3 - SIF_{num}|}{3} \tag{21}$$

The convergence diagram of the error is shown in Figure 2(b), where N is the total number of particles used for the numerical solution.

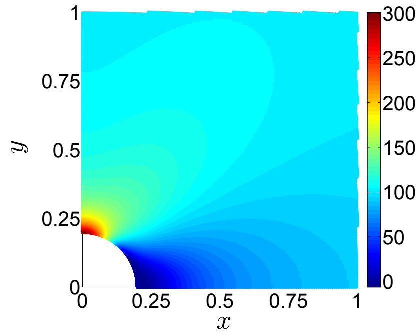

(a) σ_{xx} in a square with a central hole

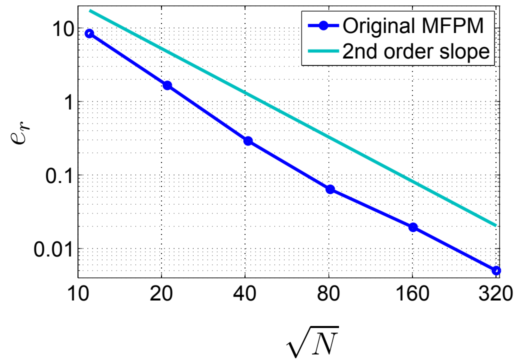

(b) Logaritmic convergence diagram of the error of the SIF in a square plate with a central hole

Figure 2: The quarter of perforated plate: numerical solution and convergence diagram

4.2 Dynamics of a bar under quasi-impulsive load

We consider a two-dimensional bar under a quasi-impulsive load. The geometry is depicted in figure 3, where $L = 1$ and $H = 0.2$.

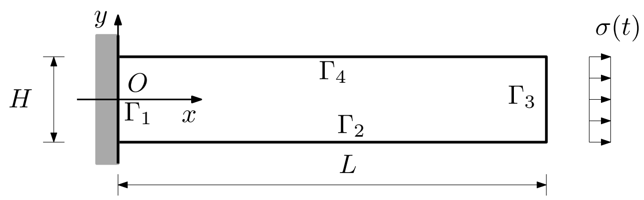

Figure 3: Geometry of the bar under quasi-impulsive load

The equations that govern the problem are the 2D plane strain version of (10); the boundary conditions are

$$\begin{cases} u = 0 & \text{and} \quad v = 0 & \text{on } \Gamma_1 \\ \sigma_{yy} = 0 & \text{and} \quad \tau_{xy} = 0 & \text{on } \Gamma_2 \text{ and } \Gamma_4 \\ \sigma_{xx} = \sigma(t) & \text{and} \quad \tau_{xy} = 0 & \text{on } \Gamma_3 \end{cases} \tag{22}$$

where $\sigma(t) = \sigma_0 \exp\left(-b(t-t_0)^2\right)$ is the quasi-impulsive load on the right side of the bar; the test has been performed considering a Poisson ratio equal to zero, so to reproduce a one-dimensional test. We also set $E = 100$ and $\rho = 100$. For this test an analytical solution is available for $\sigma_{xx}(x, y)$, since the analytical propagation speed $c = \sqrt{E/\rho}$ is known.

The missing data of this problem are:

$$\sigma_0 = -100, \qquad b = 100, \qquad t_0 = 0.3 \tag{23}$$

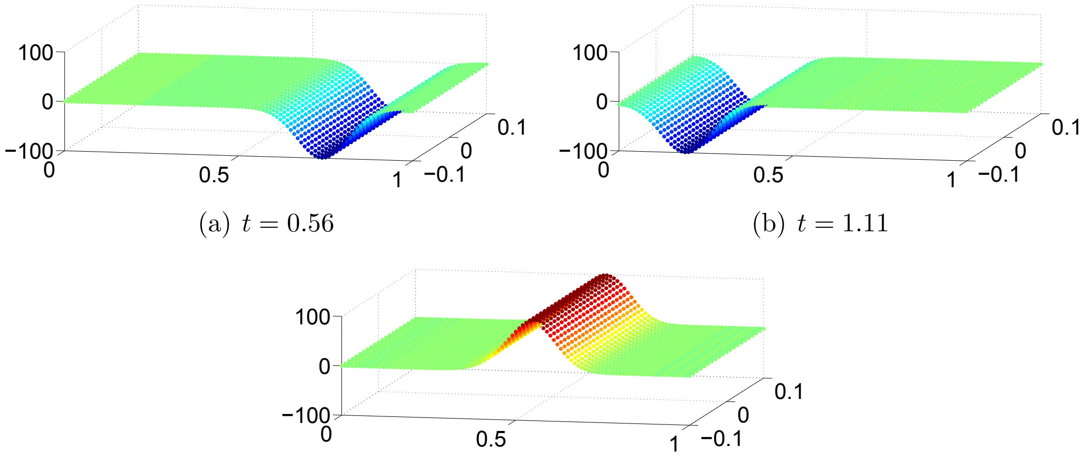

Figure 4: The stress component σ_{xx} in the bar during some time instants.

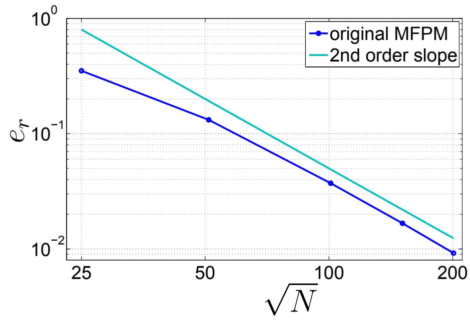

Figure 5: Convergence diagram for the bar under quasi-impulsive load

We show in Figure 5 the convergence of the error for this test. The numerical results of σ_{xx} are compared with the analytical solution after $2.5s$ from the impulse, so that the analytical reference solution is

$$\sigma_{xx}(x, y, t = 2.8) = -\sigma_0 exp\left(-b(x - 0.5)^2\right) \tag{24}$$

The relative error is

$$e_r = \frac{\|\boldsymbol{\sigma}_{xx,an} - \boldsymbol{\sigma}_{xx,num}\|}{\|\boldsymbol{\sigma}_{xx,an}\|} \tag{25}$$

4.3 Quarter of annulus under a sinusoidal body load

The geometry of this problem is depicted in Figure 6(a). The structure is clamped on all its boundary, and undergoes a sinusoidal body load. The internal radius is $r = 1$, the external one is $R = 4$.

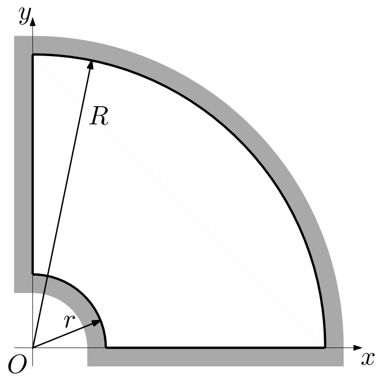

(a) Domain of the quarter of annulus with sinusoidal body load

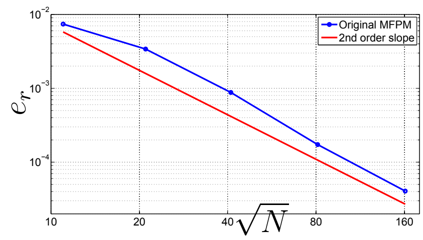

(b) Convergence diagram of the error for the quarter of annulus under sinusoidal body load

Figure 6: Quarter of annulus: geometry of the problem and convergence diagram of the error

The internal body loads and the initial conditions have been computed so that the analytical solution for the displacements u and v is

$$u(x, y, t) = v(x, y, t) = \frac{1}{100} xy(x^2 + y^2 - 16)(x^2 + y^2 - 1)\sin(2\pi t) \tag{26}$$

The relative error

$$e_r = \frac{\|u_{an} - u_{num}\|}{\|u_{an}\|} \tag{27}$$

is computed at time $t = 1.75$. The time step is $\Delta t = 10^{-4}$. In Figure 6(b) we show the rate of convergence of the error and we observe that the second-order accuracy of the method is confirmed.

5 CONCLUSIONS

In this paper we have recalled the Modified Finite Particle Method formulation for multi-dimensional problems, and have proposed its extension to dynamics. We have applied the method to an elasto-statics (a quarter of plate with a circular hole) and two elasto-dynamics (a bar under a quasi-impulsive load and a quarter of annulus under a sinusoidal body load) tests. The results obtained confirm the second order accuracy of the method for all the tests where an analytical solution was available.

Further developments will include the extension of the MFPM formulations to schemes based on a randomly distribution of particles, in order to make the method more general and suitable for application involving large deformations and fluid dynamics.

References

[1] L.B. Lucy. A numerical approach to the testing of the fission hypothesis. *The astronomical journal*, 82:1013–1024, 1977.

[2] R.A. Gingold and J.J. Monaghan. Smoothed Particle Hydrodynamics: theory and application to non spherical stars. *Monthly Notices of the Royal Astronomical Society*, 181:375–389, 1977.

[3] W. K. Liu, S. Jun, and Y. F. Zhang. Reproducing Kernel Particle Methods. *International Journal for Numerical Methods in Fluids*, 20:1081–1106, 1995.

[4] J. K. Chen, J. E. Beraun, and T. C. Carney. A corrective smoothed particle method for boundary value problems in heat conduction. *International Journal for Numerical Methods in Engineering*, 46:231–252, 1999.

[5] G.M. Zhang and R.C. Batra. Modified smoothed particle hydrodynamics method and its application to transient problems. *Computational Mechanics*, 34:137–146, 2004.

[6] D. Asprone, F. Auricchio, G. Manfredi, A. Prota, A. Reali, and G. Sangalli. Particle Methods for a 1d Elastic Model Problem: Error Analysis and Development of a Second-Order Accurate Formulation. *Computational Modeling in Engineering & Sciences*, 62:1–21, 2010.

[7] D. Asprone, F. Auricchio, and A. Reali. Novel finite particle formulations based on projection methodologies. *International Journal for Numerical Methods in Fluids*, 65: 1376–1388, 2011.

[8] D. Asprone, F. Auricchio, and A. Reali. Modified Finite Particle Method: applications to elasticity and plasticity problems. *International Journal of Computational Methods*, 2012.